Biogeosciences, 9, 5391–5406, 2012
www.biogeosciences.net/9/5391/2012/
doi:10.5194/bg-9-5391-2012

Biogeosciences

Quantitative reconstruction of sea-surface conditions over the last ∼150 yr in the Beaufort Sea based on dinoflagellate cyst assemblages: the role of large-scale atmospheric circulation patterns

L. Durantou[1], A. Rochon[1], D. Ledu[2], G. Massé[2], S. Schmidt[3], and M. Babin[4]

[1]Institut des sciences de la mer (ISMER), Université du Québec à Rimouski, 310 allée des Ursulines, Rimouski, QC, Canada
[2]LOCEAN Institut Pierre-Simon Laplace, UMR7159, 4 Place Jussieu, BP100 75252 Paris Cedex, France
[3]Université de Bordeaux, EPOC, UMR5805, 33400 Talence, France
[4]Takuvik Joint Laboratory, Université Laval, Pavillon Alexandre-Vachon, 1045, avenue de la Médecine, local 2064, Quebec city, Canada

Correspondence to: L. Durantou (lise.durantou@uqar.qc.ca)

Received: 31 March 2012 – Published in Biogeosciences Discuss.: 19 June 2012
Revised: 6 November 2012 – Accepted: 7 November 2012 – Published: 21 December 2012

Abstract. Dinoflagellate cyst (dinocyst) assemblages have been widely used over the Arctic Ocean to reconstruct sea-surface parameters on a quantitative basis. Such reconstructions provide insights into the role of anthropogenic vs natural forcings in the actual climatic trend. Here, we present the palynological analysis of a dated 36 cm-long core collected from the Mackenzie Trough in the Canadian Beaufort Sea. Dinocyst assemblages were used to quantitatively reconstruct the evolution of sea-surface conditions (temperature, salinity, sea ice) and freshwater palynomorphs fluxes were used as local paleo-river discharge indicators over the last ∼150 yr. Dinocyst assemblages are dominated by autotrophic taxa (68 to 96 %). Cyst of *Pentapharsodinium dalei* is the dominant species throughout most of the core, except at the top where the assemblages are dominated by *Operculodinium centrocarpum*. Quantitative reconstructions of sea-surface parameters display a series of relatively warm, lower sea ice and saline episodes in surface waters, alternately with relatively cool and low salinity episodes. Variations of dinocyst fluxes and reconstructed sea-surface conditions may be closely linked to large scale atmospheric circulation patterns such as the Pacific Decadal Oscillation (PDO) and to a lesser degree, the Arctic Oscillation (AO). Positive phases of the PDO correspond to increases of dinocyst fluxes, warmer and saltier surface waters, which we associate with upwelling events of warm and relatively saline water from Pacific origin. Freshwater palynomorph fluxes increased in three phases from AD 1857 until reaching maximum values in AD 1991, suggesting that the Mackenzie River discharge followed the same trend when its discharge peaked between AD 1989 and AD 1992. The PDO mode seems to dominate the climatic variations at multi-annual to decadal timescales in the western Canadian Arctic and Beaufort Sea areas.

1 Introduction

Recent observations revealed that the Arctic has experienced a warming at a rate nearly twice the global average during the past decades (e.g. IPCC, 2001, 2007; McBean, 2005; Hassol, 2004) and sea-ice extent recorded still declines, with a new minimum reached in mid-September 2012 (National Snow and Ice Data Center). Most of the climate variability over the Arctic has been associated with changes in the phase of large scale atmospheric patterns such as the Arctic Oscillation (AO) or the Pacific Decadal Oscillation (PDO) (Niebauer and Day, 1989; Macdonald et al., 2005; Overland et al., 1999; Thompson and Wallace, 1998), which are both important natural patterns in global climate variability. Unfortunately, the lack of long-term observations in the Arctic makes it impossible to reach any definitive conclusion concerning the environmental changes induced by climatic oscillations in Arctic regions (e.g. Polyakov et al., 2002). In this context, paleoceanographic studies at high temporal

resolution (i.e. multi-annual to decadal scales) were recently solicited in order to acquire a better knowledge about past and actual climate affecting high latitudes. Previous paleoceanographic studies have actually shown the relative importance of the Arctic Oscillation in the Southern Beaufort Sea during the Holocene (e.g. Bringué and Rochon, 2012; Ledu et al., 2008, 2010a, 2010b). The Arctic Oscillation is a multi-year mode of positive and negative values index reflecting anomalies in the strength of the circumpolar vortex, which is well-correlated with the interannual and decadal time scale variability in the Arctic (Thompson and Wallace, 1998). However, the actual understanding of natural variability versus the anthropogenic warming contribution, mainly based on past observations with both proxy and instrumental records still needs to be better documented at adequate temporal scales. In this paper, we present quantitative multi-year resolution (3–5 yr) reconstructions of sea-surface conditions based on dinocyst assemblages preserved in the Beaufort Sea sediments. The sediment core was collected as part of the Malina Program (http://www.obs-vlfr.fr/Malina) in an attempt to provide a paleoenvironmental perspective on the recent climatic evolution in the Beaufort Sea coastal region, which has experienced a drastic reduction of both area and thickness of sea ice cover over the last few decades (Barber and Hanesiak, 2004).

Dinocyst assemblages were used as proxy to document the quantitative evolution of sea-surface conditions. Dinoflagellates are unicellular protists, some of which producing a cyst as part of their life cycle to avoid adverse conditions (e.g. winter), and returning to their planktonic form the following season when environmental conditions improve. They are preserved in most marine sediments because of the composition of their highly resistant organic membrane, and despite extremely cold conditions (e.g. de Vernal et al., 2001; Harland and Pudsey, 1999; Rochon et al., 1999). Dinocysts are particularly useful microfossils in high latitudes because they are especially sensitive to sea-surface conditions in Arctic and sub-Arctic areas (e.g. Kunz-Pirrung, 2001; Matthiessen et al., 2005; Mudie and Rochon, 2001; Radi et al., 2001; de Vernal et al., 2001, 2005). Furthermore, dinocysts are preferentially preserved in environments like the Mackenzie Trough where sediment accumulation rates are relatively high, which prevents oxidation.

2 Study area

The Mackenzie Shelf is a 120 km wide and 530 km long area, representing approximately 6.0×10^4 km^2. It is located between the Mackenzie Trough to the west and the Amundsen Gulf to the East (Fig. 1). The water column is characterised by Pacific water masses but Atlantic water is also present at depth below 200 m. Sea ice is generally present between mid-October and the end of May (Wang et al., 2005; O'Brien et al., 2006). Among others, the Beaufort Shelf surface circulation is strongly influenced by ice (pack-ice and landfast ice), winds and freshwater inputs resulting from river discharge and sea ice melt (Carmack et al., 2004).

The water column at the core location is composed of 3 layers: the upper polar mixed layer (salinity < 28), the relatively cold lower Polar Mixed Layer (20–50 m, salinity of 28 to 30.7) (e.g. Matsuoka et al., 2012) and the-nutrient-rich relatively warm and salty Bering Summer Water below 50 m (with a salinity of ~ 31) (Carmack et al., 1989; Carmack and Macdonald, 2002; Macdonald et al., 1987) composed in part by the Alaskan Coastal water (Steele et al., 2004). The upper polar mixed layer is a combination of surrounding sea ice melt, Mackenzie River discharge, but also other processed waters (from Pacific and/or Atlantic). In this layer, primary production usually responds to nutrient inputs. Turbidity due to the Mackenzie plume between May and September and the absence of nutrients limit primary production, but a chlorophyll *a* maximum is found near 20–60 m depth (Martin et al., 2010). Offshore, the Beaufort Gyre flows clockwise while, closer to shore, the relatively warm Alaskan Coastal Current (Fig. 1) (Aagaard, 1984; Coachman et al., 1975) flows eastward throughout the year (Nikolopoulos et al., 2009) transporting the Alaskan Coastal Waters, which composed part of the halocline of the water column in the study area (Aaagard, 1984; Melling, 1998).

The Mackenzie River is the fourth largest Arctic river in terms of freshwater discharge but the first in terms of sediments discharge, which represents annually 127 Mt of sediments, and largely influenced by an ice cover, winds and currents (Carson et al., 1998; Macdonald et al., 1998). Closer to shore, the Mackenzie River freshwater inputs form a large plume (Fig. 1), dominant at the surface during summer time, which distributes water properties of the river over the Beaufort Sea surface layer (Macdonald et al., 2002; Doxaran et al., 2012). The Mackenzie River plume is typically 2–3 m thick and it is characterised by a strong vertical and horizontal structure. It is influenced by westward coastal winds toward the Mackenzie Trough and eastward surface current to the Canadian Archipelago (Carmack and Macdonald, 2002).

The Mackenzie River drainage basin covers a large part of western Canada, around 1.8×10^6 km^2 (Abdul Aziz and Burn, 2006; Hill et al., 2001), delimited by the east flank of the Rocky and Mackenzie Mountains. Highest sediment accumulation rates are found in the Mackenzie Trough and the nearby continental slope (Hill et al., 1991; Macdonald et al., 1998; Scott et al., 2008). The Mackenzie Shelf receives 249–333 km^3 of freshwater annually (Dittmar and Kattner, 2003), usually during the May–September period (Macdonald et al., 1998) but reduced in winter near the coast, underneath the land fast ice (Macdonald et al., 1995). The core is located in the progradation of the modern delta zone (Hill et al., 1996), largest distributary channels of the Mackenzie River in the Mackenzie Trough where sedimentation rates of few millimeters per year can be observed (e.g. Scott et al., 2009; Bringué and Rochon, 2012), which are largely higher than sedimentation rates found in other Arctic regions

(e.g. Ledu et al., 2008; Rochon and de Vernal, 1994). Coastal erosion represents around 7 Mt yr^{-1} over the shelf (Macdonald et al., 2002.) depending on the Mackenzie River flow intensity and storms.

The main part of the Mackenzie Trough is composed of silty sediments, while the nearby shelf is mostly characterised by silt and sand (Barletta et al., 2008; Blasco et al., 1990; Hill 1996, 2001; Jerosh et al., in press; Scott et al., 2009). The morphology of the Mackenzie Trough, together with strong winds and ice dynamics, can cause upwelling of the warmer and saltier Pacific halocline (Aagaard, 1984). These conditions occur over the trough, shelf area and along the slope, and many were observed over the last 4 decades (Carmack et al., 1989; Carmack et al., 2004; Iseki et al., 1987; Kulikov et al., 1998; Macdonald et al., 1987; Williams et al., 2006). From a year-to-year comparison, periods with no upwelling conditions are characterised by lower sea-surface primary production (Macdonald et al., 2002). Both ice-motion and ice-free conditions allow the development of upwelling events, which are observed in both winter and summer seasons.

3 Material and methods

3.1 Sampling and preparations

The 36 cm-long core MA680BC (69°36′15″ N, 138°13′34″ W) studied here was collected during the 2009 Malina sampling campaign onboard the CCGS *Amundsen* with a box corer at 125 m water depth (Fig. 1). The core was sub-sampled at 1 cm intervals and treated using standardized palynological procedures (e.g. Rochon et al., 1999) involving chemical treatments. To that end, 5 cm^3 of sediments were collected by water displacement and a tablet of marker grains (*Lycopodium clavatum*, University of Lund, Sweden) of known concentration (12 100 spores ±1892 spores/tablet, Batch n° 414 831) was added to the sediments, allowing calculation of palynomorph concentrations (Matthews, 1969). Sieving at 10 and 100 µm was performed in order to eliminate fine and coarse particles (< 10 µm and > 100 µm). This was followed by warm acid treatments using hydrochloric acid (HCl-10 %, 4 treatments) to dissolve the carbonated particles alternating with hydrofluoric acid to dissolve the silicate particles (HF-49 %, 3 treatments). A final sieving was realised (10 µm) to eliminate fine particles and fluorosilicates formed during the chemical treatments. Finally, a drop of the residue was mounted between slide and coverslip in glycerin gel.

3.2 Dinocyst counts

Slides were observed in transmitted-light microscopy (Leica, DM5500B) at 400x magnification. All palynomorphs (pollen, spores, dinocysts, freshwater palynomorphs, organic linings of foraminifera, acritarchs and pre-Quaternary palynomorphs) were systematically counted in each sample. A minimum of 300 dinocysts were counted to obtain a significant statistical representation of the dinocyst populations. Relative abundances were calculated from the dinocyst sum, and fluxes (specimens $cm^{-2}\,yr^{-1}$) were calculated based on concentrations (cysts cm^{-3}) and the ^{210}Pb-based sediment accumulation rates (cm yr^{-1}). The low oxidation level was evidenced by the excellent preservation of the most oxidation-sensitive taxa (Zonneveld et al., 1997), such as those of the genus *Brigantedinium*.

3.3 Modern Analog Technique – estimation of past sea-surface conditions and taxonomy considerations

The reconstruction of past sea-surface conditions was done using the Modern Analogue Technique (MAT) (Guiot et al., 1990; Prell, 1985; de Vernal et al., 2001, 2005) with the statistical software R version 2.13.0. The MAT is routinely used and particularly well-suited for the reconstruction of past sea-surface conditions in high-latitude environments (Bonnet et al., 2010; Guiot and de Vernal, 2007, 2011; Ledu et al., 2010). Here we also use the "bioindic" package built on the R-platform (http://cran.r-project.org/) (Gally and Guiot), especially designed to offer various types of statistical analyses such as multivariate analyses, times series analyses, spatial analyses, tree-ring analyses, and transfer functions. The MAT method is based on the similarity between fossil dinocyst spectra and modern analogs from a large reference database DS-1419 (= 1419 data sites, GEOTOP). Data of surface sediment dinocysts distribution in the Northern Hemisphere are available on the GEOTOP website (http://www.geotop.ca/en/bases-de-donnees/dinokystes.html) and validation tests were applied on the database DS-1419 (Bonnet et al., 2012), confirming the suitability of the MAT method in paleonvironmental reconstruction studies. Modern sea-surface temperature (SST) and sea-surface salinity (SSS) (at 10 m depth) are respectively from the World Ocean Atlas (NODC, 2001) and ArcticNet 2009 data. The modern sea ice cover values (SIC) used are from 1953–1990 data of the National Snow and Ice Data Center (number of months per year with > 50 % of sea ice cover), and reconstructions performed on dinocyst assemblages were also compared with sea ice cover variations available from HADISST.

Data for the Mackenzie River discharge are from the Environment Canada website, and viewed with HYDAT software (ftp://arccf10.tor.ec.gc.ca/wsc/software/HYDAT/). Mean annual discharge is compiled from 3 stations data for the period 1972–2005, 2 stations data for the period 1943–1972, and 1 station from 1938–1943. Data from the AO and the PDO are annual averages from the National Oceanic and Atmospheric Administration (NOAA).

Dinocyst nomenclature follows that of Rochon et al. (1999), de Vernal et al. (2001), Head et al. (2001), Radi et al. (2001), Fensome and Williams (2004) and Radi et al. (2012). The following taxa are grouped together with

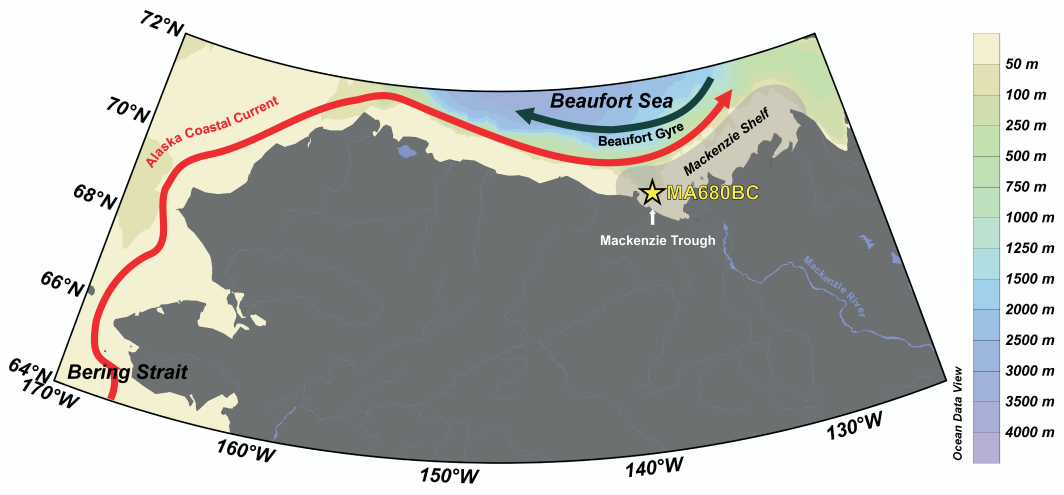

Fig. 1. Location map of core MA680BC and oceanic circulation in the study area. The black arrow represents the clockwise Beaufort Gyre, the red arrow indicates the Alaska Coastal Current and the grey area represents the Mackenzie River plume.

Islandinium minutum because they often co-occur in samples and their individual ecologies are still unknown: *Islandinium brevispinosum* (Fig. 2i), *Echinidinium karaense* (Fig. 2k), *Echinidinium zonneveldiae*, *Echinidinium granulatum* and *Echinidinium* sp. *Z. Spiniferites elongatus*, *S. frigidus* and intergraded morphotypes are also grouped together (Rochon et al., 1999).

3.4 Palynomorph counts

Other palynomorphs include pollen and spores, freshwater palynomorphs, which include *Pediastrum* (Fig. 2a), *Halodinium* (Fig. 2b) and spores of *Zygnema* (Fig. 2c), acritarchs and pre-Quaternary palynomorphs. The concentrations of these palynomorphs were expressed in terms of fluxes (specimens $cm^{-2}\,yr^{-1}$). Freshwater palynomorphs are identified at the genus level and are used as indicators of freshwater input from the Mackenzie River (Matthiessen et al., 2000). Acritarchs and pre-Quaternary palynomorphs, which include dinocysts, pollen grains and spores, are used as sediment reworking indicators (de Vernal and Hillaire-Marcel, 1987).

3.5 Chronology and grain size analysis

The chronological framework of core MA680BC was determined based on ^{210}Pb excess and ^{137}Cs. Activities of ^{210}Pb, ^{226}Ra and ^{137}Cs excess were measured in the UMR5805 EPOC-OASU laboratory using a low background, high-efficiency, well-shaped γ detector (Schmidt et al., 2009). Calibration of the γ detector was achieved using certified reference materials (IAEA-RGU-1; IAEA-RGTh; SOIL-6). Activities are expressed in $mBq\,g^{-1}$ and errors are based on 1 SD counting statistics. Excess ^{210}Pb was calculated by subtracting the activity supported by its parent isotope, ^{226}Ra, from the total ^{210}Pb activity in the sediment. Errors in $^{210}Pb_{xs}$ were calculated by propagation of errors in the corresponding pair (^{210}Pb and ^{226}Ra). Use of the naturally-occurring ^{210}Pb has been widely done to calculate short-term (years to decades) sediment accumulation rates in continental and oceanic environment since the last 40 yr (Appleby, 2001). Dating is calculated using excess activity of ^{210}Pb ($^{210}Pb_{xs}$), which is incorporated rapidly into the sediment from atmospheric fallout and water column scavenging. Once incorporated into the sediment, unsupported ^{210}Pb decays with time, in the sediment column according to its half-life and Eq. (1):

$$^{210}Pb_{xs(z)} = {}^{210}Pb_{xs(0)}e^{-\lambda t} \quad (1)$$

where $^{210}Pb_{xs(0)}$ and $^{210}Pb_{xs(z)}$ represent the excess ^{210}Pb at the sediment-water interface, or at the base of the mixed layer, and at the depth z, λ is the ^{210}Pb decay constant ($0.0311\,yr^{-1}$), and t is the age in years. Several models have been developed to calculate an age or accumulation rate: CIC (constant initial concentration), CRS (constant rate of supply), CFCS (constant flux-constant sedimentation) (e.g. Sanchez-Cabeza and Ruiz-Fernández, 2012). The CRS model was chosen for core MA680BC (Fig. 6). The accuracy of this ^{210}Pb-based age model was checked using an independent time-stratigraphic marker, the fallout ^{137}Cs ($T_{1/2} = 30$ yr).

Grain size measurements on the box core were realised with a Beckman-Coulter laser diffraction analyser (LS-13320) at ISMER with a 1 cm interval and statistical grain size distribution was computed with the Gradistat software (Blott and Pye, 2001).

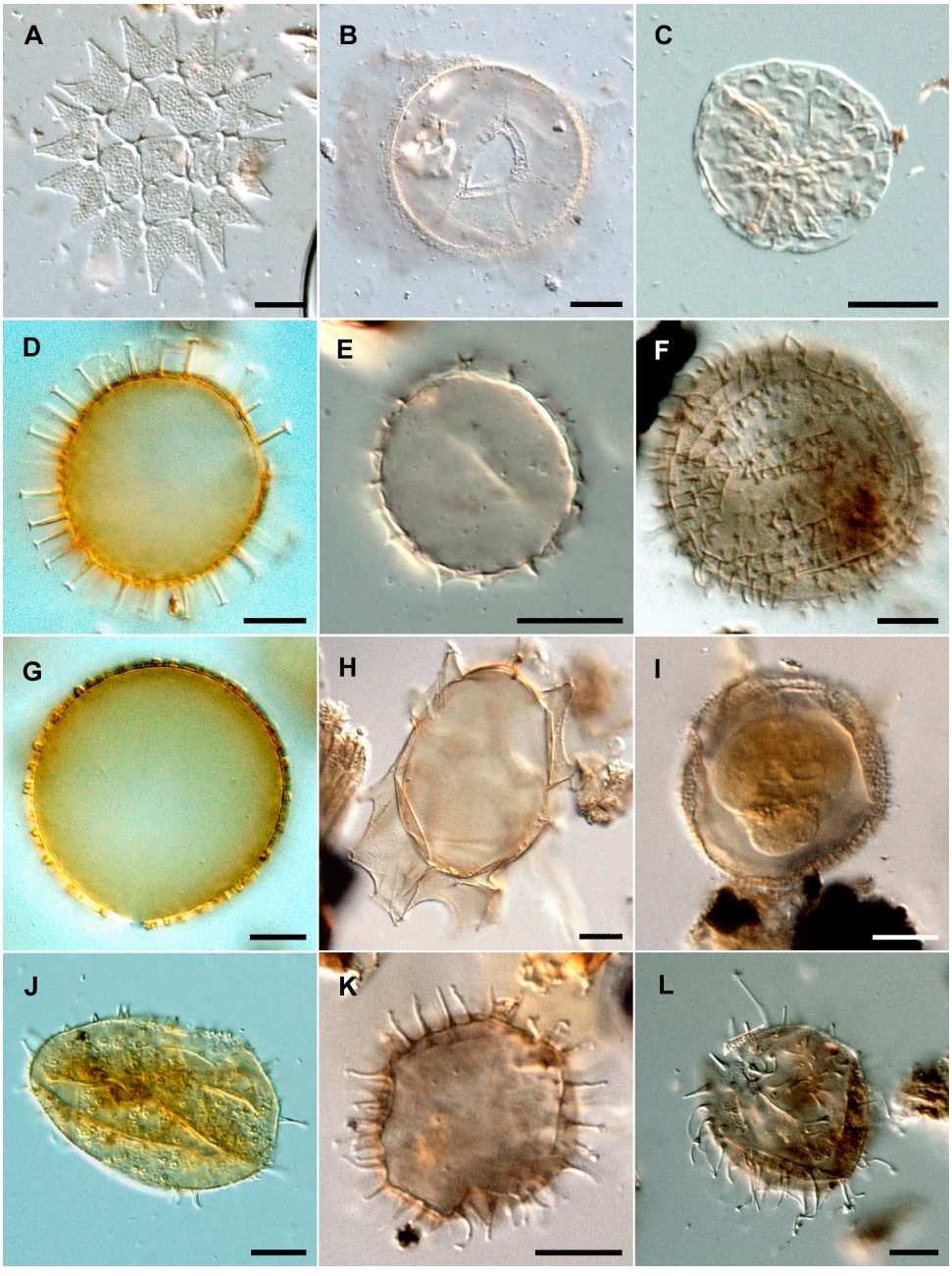

Fig. 2. The scale bar represents 10 µm. **A.** *Pediastrum* sp. **B.** *Halodinium* sp. **C.** *Zygnema* sp. **D.** *Operculodinium centrocarpum* **E.** Cyst of *Pentapharsodinium dalei* **F.** *Islandinium minutum* **G.** *Operculodinium centrocarpum* short spines **H.** *Spiniferites frigidus* **I.** *Islandinium brevispinosum* **J.** *Operculodinium centrocarpum* var. Arctic **K.** *Echinidinium karaense* **L.** *Islandinium cezare*.

4 Results

4.1 Grain size and chronology

Overall, the mean grain size profile is defined as poorly sorted mud to fine-silt sediment along the core. The Silt/Clay ratio reach more than 2/1 for most samples corresponding with Mackenzie Trough and prodelta slope sediment characteristics (Hill et al., 2001; Jerosch et al., 2012; Pelletier, 1984; Scott et al., 2009).

^{210}Pb excess activities range from 3 to 82 m Bq g^{-1}. There is a general trend in decreasing $^{210}Pb_{xs}$ as expected due to the decay with depth of the unsupported ^{210}Pb. This decrease presents some irregularities, as observed at about 16–18 cm along with a slight change in dry bulk density, where excess is lower when compared to the surrounding layers. This

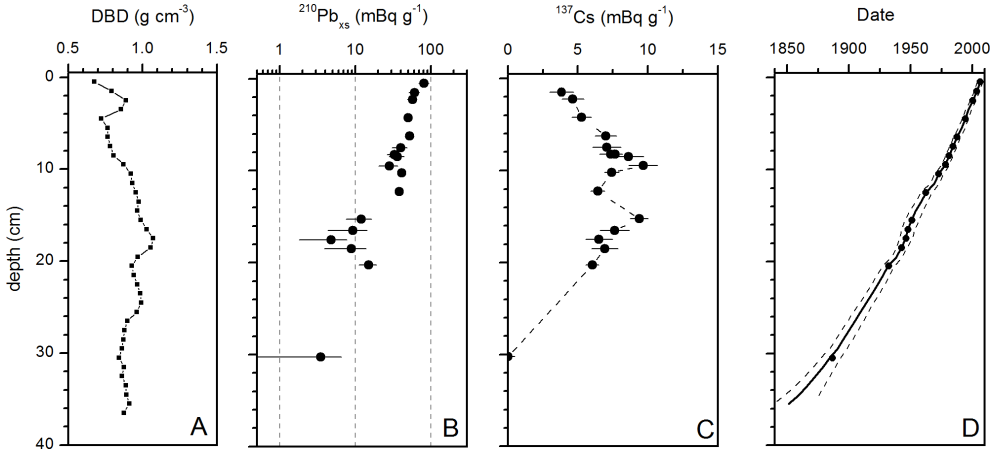

Fig. 3. Dry bulk density **(A)**, ^{210}Pbxs **(B)**, ^{137}Cs profiles **(C)** and ages of sedimentary 1032 layers, based on CRS model, **(D)** with depth in core MA680BC.

could be in relationship with a temporary changes in sedimentation (intensity or nature of sediment) that justifies the use of the CSR model for dating. The 36 cm-long core encompasses the last 150 yr. ^{137}Cs profile in core MA680BC shows the two expected peaks in activity (Fig. 3), in agreement with the well-known pulse inputs related to the nuclear weapon test fall-out in the early sixties (maximum atmospheric fallout in 1963 in the Northern Hemisphere), and to the Chernobyl accident in 1986 (UNSCEAR, 2000). The calculated sediment accumulation rates range from 0.32 cm yr^{-1} in the upper part of the core to 0.22 cm yr^{-1} at the base of the sequence, allowing for a multi-annual resolution of 3–4 yr throughout the record (Fig. 3). Sedimentation rate in core MA680BC is in the expected range for a shelf submitted to river discharges.

4.2 Palynomorph fluxes

Dinocyst concentrations varied between 700 and 2400 cysts cm^{-3} (average 1500 cysts cm^{-3}) and are of the same order of magnitude than those previously found in surface sediments from the Beaufort Shelf area (200–3100 cysts cm^{-3}) (Richerol et al., 2008b). Because dinoflagellate productivity in estuarine zones is not necessarily reflected in assemblages and heterotrophic/autotrophic ratio (Radi et al., 2007), in the present study we are presenting dinocyst results as flux to better convey changes in dinoflagellate primary productivity throughout the time period covered by our core. Dinocyst fluxes (Fig. 4) vary between 200 and 1400 cysts cm^{-2} yr^{-1} (average 500 cysts cm^{-2} yr^{-1}). From ∼AD 1865–1910, fluxes increase gradually from 300 to 750 cysts cm^{-2} yr^{-1}), with a first maximum around AD 1910. Around AD 1920, a slight minimum of 450 cysts cm^{-2} yr^{-1} is observed, followed by a slight maximum around AD 1930 of 1000 cysts cm^{-2} yr^{-1}. Between ∼AD 1930–1970, dinocysts fluxes are decreasing, with a minimum value reached around AD 1950 (200 cysts cm^{-2} yr^{-1} at 14 cm downcore) and increase again from AD 1970–1980 to reach a maximum value of 1400 cysts cm^{-2} yr^{-1} at 8 cm downcore. Dinocyst fluxes then steadily decrease from ∼AD 1980 to their modern value of 400 cysts cm^{-2} yr^{-1} at the top of the core. Pollen and spore fluxes (Fig. 4) remain relatively stable during ∼AD 1855–1950 with a mean value of 267 grains cm^{-2} yr^{-1}, despite a peak centered ∼AD 1900. From AD 1950, fluxes progressively increase to reach a maximum value of 660 grains cm^{-2} yr^{-1} during ∼AD 1980–2000, with a mean value of 580 grains cm^{-2} yr^{-1}. Principally 5 genus composed the pollen assemblages: *Picea*, *Pinus*, *Betula*, *Alnus* and *Salix*, and the assemblage is represented by 30–80 % of trees, 5–36 % of shrubs and only 0–10 % of herbs. *Pinus* dominated the assemblages and it is generally over-represented in ocean basins due to its morphology, its density and its high rate of pollen grains production, which allows transport over long distances (e.g. Heusser, 1983; Mudie, 1982; Rochon and de Vernal, 1994). Fluxes of pollen and spores and pre-Quaternary palynomorphs (pollen grains, spores and dinocysts) present similar distribution patterns. Fluxes are minimum ∼AD 1880 (210 and 190 specimens cm^{-2} yr^{-1}, respectively) and gradually increase until ∼AD 1980. They are then characterised by an important increase between ∼AD 1980–2000 and reach maximum values of 660 and 915 specimens cm^{-2} yr^{-1}, respectively (Fig. 4b and 4c). Freshwater palynomorphs (Fig. 6d), pollen grains (Fig. 6b) and spores, and pre-Quaternary palynomorphs fluxes (Fig. 6c) are all characterised by an increase from minimum values around ∼AD 1885 to maximum values during ∼AD 1992–1997.

Freshwater palynomorphs are used as tracers for the variations of the Mackenzie River discharge (Fig. 6f). Their fluxes gradually increase from minimum values

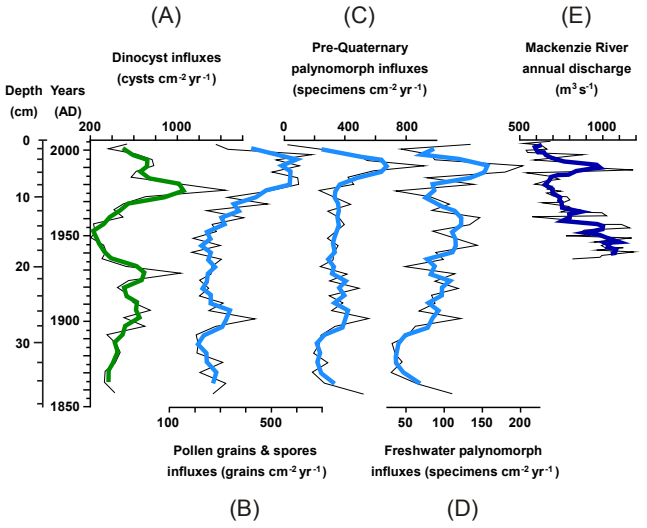

Fig. 4. Palynomorph fluxes in core MA680BC plotted against depth and age AD. Dinocyst fluxes **(A)**; Pollen and spores fluxes **(B)**; pre-Quaternary palynomorph fluxes **(C)**; freshwater palynomorph fluxes **(D)**; Mackenzie River annual discharge from 1938 to 2006 (HYDAT) **(E)**. The thick curves represent a running average over 3 data points.

of ~ 30 specimens $\mathrm{cm}^{-2}\,\mathrm{yr}^{-1}$ around AD 1880 to maximum values of 200 specimens $\mathrm{cm}^{-2}\,\mathrm{yr}^{-1}$ in the period $\sim$ AD 1980–2000. The determination coefficient computed between the Mackenzie River annual discharge and the freshwater palynomorphs fluxes is about $R^2 = 0.38$, indicating that a correlation exit between these two variables.

4.3 Dinocyst assemblages

A total of 24 dinocyst taxa were observed, but 7 taxa comprised more than 95 % of the assemblages (Fig. 5). The assemblages are dominated by the cyst of the autotrophic taxa *Pentapharsodinium dalei* (Fig. 2; E) and the taxa *Operculodinium centrocarpum* sensu lato (Fig. 2; D, G, J), which includes the arctic and short spines morphotypes. Both taxa are common in Arctic and sub-Arctic regions (Mudie and Rochon, 2001; Kunz-Pirrung et al., 2001) and were recorded in estuarine environments (Dale, 1976; Persson et al., 2000). Cyst of *P. dalei*, which represents 68 to 96 % of the assemblages, is generally associated with low salinity environments and stratified waters in summer. The second most abundant taxa, *O. centrocarpum* sensu lato, is ubiquitous in middle to high latitudes and represents 9–66 % of the assemblages (average 31 %). The accompanying taxa include *Spiniferites elongatus*/*frigidus* and a series of heterotrophic taxa: *Islandinium minutum* sensu lato (2–18 %), *Brigantedinium simplex* (1–30 %), the cyst of *Polykrikos* var. arctic (≤ 3 %) and the cyst of *Protoperidinium americanum* (≤ 2 %).

The DOS program Zone Version 1.2 (http://www.staff.ncl.ac.uk/staff/stephen.juggins/software/ZoneHome.htm) allowed to differentiate three dinocyst assemblage zones, which can also be distinguished on the basis of the relative abundance of all taxa: Dinocyst assemblage zone 1 encompasses the period $\sim$ AD 1855–1880 (Fig. 6), and is characterised by the co-dominance of cyst of *P. Dalei* (34–56 %) and *O. centrocarpum* sensu lato (28–46 %), accompanied by *S. elongatus/frigidus* (2–4 %) (Fig. 2, H), *I. minutum* sensu lato (5-17%) and *B. simplex* (3-10%). Dinocyst assemblage zone 2 encompasses the period $\sim$ AD 1880–1987 and is dominated by the cyst of *P. dalei* (24–73 %), *O. centrocarpum* sensu lato (9–46 %), while *S. elongatus*/*S. frigidus* (0.3–3 %) show their minimum relative abundances in this zone. Conversely, the assemblage is characterised by the maximum abundance of heterotrophic taxa, such as *I. minutum* sensu lato (up to 24 %) and *B. simplex* (up to 20 %), and by the appearance of cysts of *P. americanum* (0.3–2 %) and cysts of *Polykrikos* var. arctic (0.3–3 %); Dinocyst assemblage zone 3, from AD 1987–2009, is characterised by a marked decrease of cyst of *P. dalei* abundance (from 46 to 11 %) and dominance of *O. centrocarpum* sensu lato (up to 65 %). This assemblage is also marked by the maximum abundance of *S. elongatus*/*frigidus* (up to 5 %), the minimum abundance of all heterotrophic taxa and the disappearance of the cyst of *P. americanum.*

4.4 Reconstruction of sea-surface conditions

Summer SST reconstructions (Fig. 6c) are characterised by a decreasing trend between $\sim$ AD 1855–1960 and reconstructed SST between $\sim$ AD 1885–1935 are warmer by up to 3 °C with respect to the average modern temperature at the coring site which is $\sim 4.1°$ C. During $\sim$ AD 1935–1975 reconstructed SSTs are ~ 1 °C below the modern value. Within the next 10 yr, the temperature increases up to 5.4 °C ($\sim$ 1987) and gradually decreases towards the modern value of 4.1 °C.

The reconstructed SIC trend mirrors that of reconstructed SSTs (Fig. 6b). The root mean squared error (RMSE) calculated on SIC values, which is the difference between reconstructed and observed values, is 1.43 months yr^{-1}, and reflects the accuracy of the approach. For the period $\sim$ AD 1887–1945, reconstructed SIC values are on average 8.3 months yr^{-1} which is 1.1 months yr^{-1} lower than the modern values. In contrast, the period AD 1945–1975 is marked by reconstructed SIC values closer to the modern conditions, with an average value of 8.8 months yr^{-1}. A decrease in SIC characterises the period AD 1975–1995, with an average value of 7.6 months yr^{-1}, which is 1.8 months yr^{-1} below the modern value. Sea ice cover duration then gradually increases toward the modern value. All above reconstructed values are within or very close to the confidence limits of the method.

Reconstructions of SSS depict a series of oscillations between minimum and maximum values varying between −7 and +5 around the modern salinity of ∼ 27 (Fig. 6d), which is the averaged value measured from 17 stations in 2009, all located within 30 km of the coring site. The intervals from AD 1860–1905, 1935–1980 and 1990–2009 are characterised by reconstructed SSSs lower than the modern value, while SSS is similar to modern conditions between AD 1905 and 1935. The most salient feature of the reconstructions is the sharp peak recorded by all reconstructed parameters during ∼ AD 1980–1990.

5 Discussion

^{210}Pb revealed high sedimentation rates (0.2–0.3 cm yr^{-1}) directly linked to high sediment discharge from the Mackenzie River. Even if neighbouring studies using ^{210}Pb and ^{137}Cs dating in the Mackenzie Shelf area gave away lower sedimentation rates (Bringué and Rochon, 2012; Richerol et al., 2008a), results on core MA680BC core dating results are similar to other cores located on the slope between the Mackenzie Trough and the Amundsen Gulf (Scott et al., 2009). The heterogeneity of sedimentation rates in the Mackenzie Trough is caused by the dominant eastward transport of sediment in the suspended sediment plume (Hill et al., 1991).

Instrumental data for the Mackenzie River discharge were collected since 1938, which allows for short time scale observations on the fluctuations of the freshwater discharge. In an attempt to trace the temporal variability of freshwater inputs to the Beaufort Sea area prior to 1938, Richerol et al. (2008a) previously showed the similarities between concentrations of the freshwater palynomorph *Halodinium*, a thecamoeban-like palynomorph, and the Mackenzie River discharge in the Beaufort Sea area. Here, we have used the fluxes of several freshwater palynomorphs, including *Halodinium*, as well as remains of the freshwater algae *Pediastrum* (Chlorophyceae) and *Zygnema* (Zygnematophyceae). Figure 4d illustrates the fluxes of these palynomorphs next to the Mackenzie River discharge (Fig. 4e) data from 1938 to 2005. Because of the similarity between both profiles, we suggest that the fluxes of these freshwater palynomorphs can be used as tracers of the Mackenzie River discharge prior to instrumental data, which is directly related to precipitations within its catchment area. The Mackenzie discharge data are averaged values from 3 stations collected since 1938, with exception of the period 1938–1943 where data from only one station are available. Therefore, these early data must be interpreted with caution compared to the rest of the data set.

The freshwater palynomorph fluxes curve (Fig. 6f) displays 3 major phases: from AD 1858–1902 where freshwater palynomorph fluxes are minimum (∼ 50 specimens cm^{-2} yr^{-1}); an intermediate phase from AD 1900–1976 (∼ 100 specimens cm^{-2} yr^{-1}); and the most recent phase, from AD 1976–2004, where their fluxes reach maximum values (∼ 130 specimens cm^{-2} yr^{-1}). Previous studies of tree ring records from central Canada (Case and Macdonald, 1995; Sauchyn and Beaudoin, 1998; Sauchyn and Skinner, 2001), Yellowknife and the Mackenzie delta area (Pisaric et al., 2007, 2009; Porter et al., 2009) going as far back as 1505 can be used to infer precipitations and assess the variability of freshwater inputs from the Mackenzie River. Reconstruction of August–July annual precipitations in two regions of the western Canadian Prairies (western Saskatchewan) indicate that the period 1850–1900 was characterised by drought or low-precipitation episodes lasting several years, the most severe occurring between ∼ 1860–1875 (Case and Macdonald, 1995), 1880–1900 (Sauchyn and Beaudoin, 1998, Sauchyn and Skinner, 2001), and 1842–1877 in the Eastern Rocky Mountains (St George et al., 2009). For the Yellowknife area, June precipitation reconstructions indicate a negative anomaly (low precipitations) during 1850–1890, which coincides with a particularly low level stand of lake Athabasca (Stockton and Fritts, 1973) and low river levels in northern Saskatchewan (Case and Macdonald, 1995). For the Mackenzie delta region, the tree-ring width index for the period 1850–1900 displays relatively low values (Pisaric et al., 2007), and it also corresponds with the 1855–1880 positive northern Hemisphere summer temperature anomaly (Brohan et al., 2006). The minimum values of freshwater palynomorph fluxes in our record during AD 1855–1900 (∼ 30 specimens cm^{-2} yr^{-1}), coupled with the relatively high sea-surface temperature reconstructions during AD 1855–1890 (up to 3 °C above the modern value) correlate very well with these records and strongly suggest that the Mackenzie River discharge was at a minimum level. The intermediate phase of our freshwater palynomorph record (AD 1902–1976; ∼ 100 specimens cm^{-2} yr^{-1}) corresponds to a relatively wet period, during which the population census divisions in the Prairies doubled (Government of Canada, 1938), and which was also marked by more favorable climatic conditions for crop production until the 1970s. Indeed, the 20th century began with a wet period (1900–1920) (Sauchyn and Beaudoin, 1998; Watson and Luckman, 2006), as indicated by the Palmer Drought Severity Index (drought index), which was often positive during that period (Sauchyn and Skinner, 2001). The most recent phase during AD 1976–2004 (∼ 130 specimens cm^{-2} yr^{-1}) is marked by maximum fluxes of freshwater palynomorphs (Fig. 6f). The climate during this interval is well documented with instrumental data and displays the highest annual Mackenzie River discharge values on record (between 700 and 11 900 m^3 s^{-1}), with a maximum reached in 1990. The Mackenzie Trough area is thus clearly affected by freshwater inputs from the Mackenzie River (Rawlins et al., 2009), which are probably controlled by regional and global oceanic and atmospheric (precipitations) circulation patterns, such as the PDO.

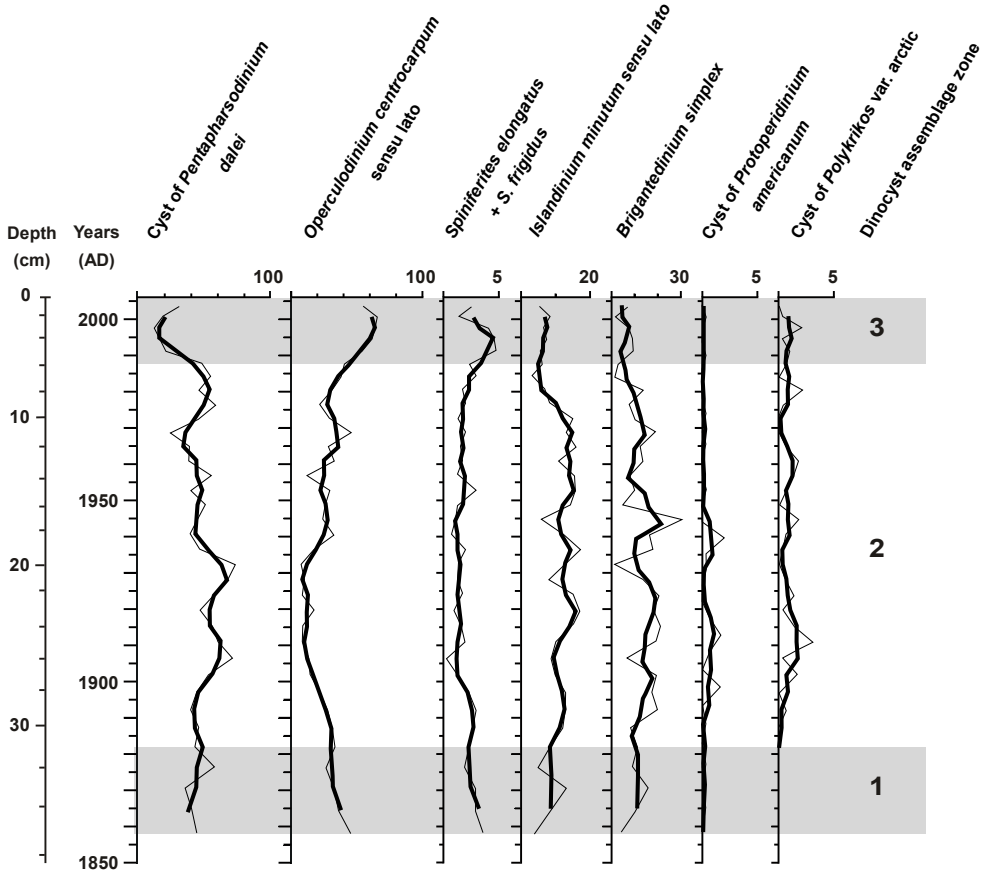

Fig. 5. Relative abundances of the main dinocyst taxa in core MA680BC and dinocyst assemblage zones plotted against depth and age AD. The thick curves represent a running average over 3 data points.

The PDO is a major mode of North Pacific climate variability and is reflected in the evolution of North Pacific monthly surface temperatures (Mantua et al., 1997; Mantua and Hare, 2002; Minobe, 1997). During positive phases, it manifests itself by low sea-level pressure anomalies over the North Pacific and high sea-level pressure anomalies over western North America. At the same time, the surface air temperatures tend to be anomalously cool in the central North Pacific and anomalously warm along the west coast of North America. The PDO also affects low pressure centers like the Aleutian Low system, which controls most of the daily precipitations in the Mackenzie and Yukon River basin (Cassano and Cassano, 2010) and the Bering Sea oceanic advection (Danielson et al., 2011). Moreover, the most recent variations of the position and intensity of the Aleutian Low centered above the Gulf of Alaska are linked with the PDO pattern (Moore et al., 2003; Schneider and Cornuelle, 2005). The Aleutian Low has been shown to deepen during positive phases of the PDO (Bjerknes, 1966, 1969, 1972; Overland et al., 1999). These regime shifts have many environmental impacts, like sea ice cover anomaly in the Bering Sea during PDO positive phases (Niebauer and Day, 1989; Niebauer, 1998). On the other hand, Aleutian Pacific-born storms (and especially northward trending trajectories storms) have many impacts in oceanic environments along the Beaufort Shelf. They generally induce upwelling events and intrusions of warmer waters through the Alaskan Coastal Current onto the Beaufort Shelf area (Okkonen et al., 2009; Pickart et al., 2009).

Along the period studied here, we can observe episodes where relatively high values of dinocyst fluxes are synchronous to relatively high SSS and SST values and relatively low values of SIC (Fig. 4b, e). Moreover, the reconstructions of sea-surface parameters for the time-period covered by the core show SSTs and SSSs above modern values during positive phases of the PDO: AD 1886–1912; AD 1925–1946 and AD 1979–1996 (Fig. 6e). Such reconstructed values are associated with upwelling conditions (warmer and saltier surface waters) on the Mackenzie Shelf during the time periods ∼ AD 1900–1910, ∼ AD 1925–1940 and ∼ AD 1980–1990. Thereby, we hypothesise that the reconstructed sea-surface parameters, coupled with dinocyst fluxes data could reflect upwelling events of saltier and warmer Pacific water recorded during positive phases of

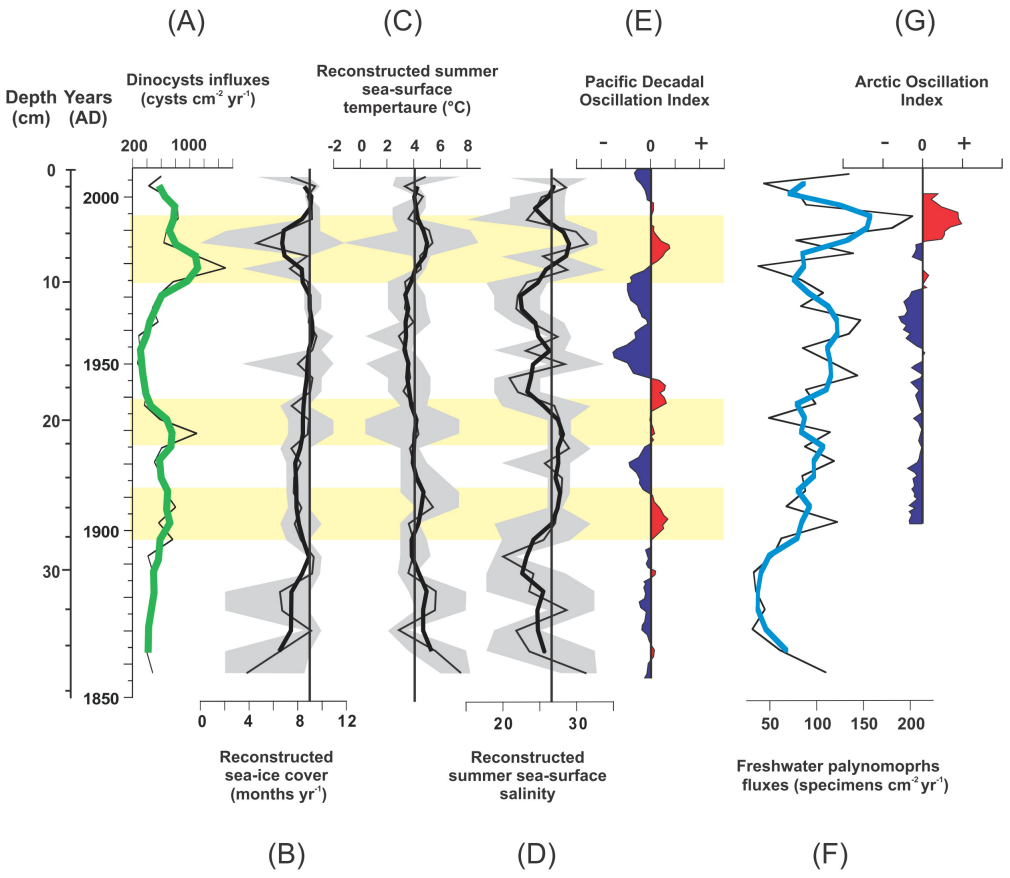

Fig. 6. Dinocyst fluxes and reconstructed sea-surface parameters in core MA680BC, and climate indexes plotted against depth and age AD. Dinocysts fluxes **(A)**; reconstructed sea ice cover **(B)**; reconstructed temperature **(C);** reconstructed salinity **(D)**; Pacific Decadal Oscillation (PDO) normalised index **(E);** freshwater palynomorph fluxes **(F);** Arctic Oscillation (AO) normalised index **(G)**. The modern values of sea-surface parameters are represented by the vertical line. The grey areas represent the confidence interval (minimum and maximum possible values) for each reconstructed parameter. The horizontal yellow areas represent warm intervals associated with positive and negative phases respectively for the PDO index (Mantua and Hare, 2002). The thick curves represent a running average over 3 data points. Both PDO and AO indexes are averaged over 5 data points.

the PDO in the Mackenzie Trough area (e.g. Macdonald et al., 1987).

Indeed, upwelling conditions observed over the Mackenzie Shelf and Trough areas have several impacts on the local productivity, such as the production of ice algae, phytoplankton, zooplankton and benthos (Tremblay et al., 2011) and affect the carbon cycle (Mucci et al., 2010). Along the core, the dinocyst assemblages are mostly composed of autotrophic taxa. The high abundance of the cyst *P. dalei*, generally associated with stratified waters and productivity (e.g. Solignac, 2009; Marret et al., 2004) is also found in advection zones of warmer and salty water as the Sassenfjorden (Grøsfjeld et al., 2009). Recent study in Rijpfjorden (Svalbard) by Howe et al. (2010) highlighted the presence of this taxon with relatively low abundance of round brown *Protoperidinium* cysts and *S. elongatus/frigidus*, providing evidences of late autumn and summer cyst production. In the same way, the relative abundance of *O. centrocarpum* sensu lato can be associated with advection of warm saline waters, accompanied by the relatively low abundances of the taxa *I. minutum*. Here, dinocysts assemblages are marked by high abundance of the cysts of *P. dalei* and *O. centrocarpum*, accompanied by relatively low abundances of round brown *Protoperidinium* cysts and *S. elongatus/frigidus*. In this case, the relatively short studied time period does not allow long-term observations, but variations of the abundance of *I. minutum* could also be related to the abundance of *O. centrocarpum* along the core. For the time being, the presence of the cysts *P. dalei* here is not linked to eutrophication as it is on the west coast of Sweden (Harland et al., 2006) or in the Oslo fjord (Dale et al., 1999) and anthropogenic effects are not evidenced in the studied area. Furthermore, relationships between dinocyst abundance (percentage or fluxes) and nutrient concentrations, or paleoproductivity, were observed in other upwelling regions (Zonneveld and Brummer, 2000; Wendler et al., 2009; Susek et al., 2005). The reconstructed

paleoproductivity values provided by the MAT method were not used because instrumental data in the Beaufort Sea area are scarce, causing the reconstructions to be unreliable. Therefore, we used dinocyst fluxes as indicators of paleoproductivity. Dinocyst fluxes are relatively high during the period ∼ AD 1900–1910 but more important during the periods ∼ AD 1925–1940 and ∼ AD 1980–1990, synchronous with higher than present SST and SSS estimates and lower SIC duration, consistent with an increase of primary productivity caused by upwellings of Pacific water in the Mackenzie Trough area. Conversely, we observe relatively low dinocyst fluxes during most negative phases of the PDO (∼ AD 1910–1925; ∼ AD 1995–2005, and ∼ AD 2000). A study by Ledu et al. (unpublished) on core MA680BC based on lipid compounds production by sea ice algae (IP_{25}) indicated a close relationship between the PDO index and sea ice productivity. They attributed the enhancement of sea ice primary productivity to the increased frequency of upwelling events of warm and salty Pacific waters along the Beaufort slope during positive phases of the PDO. However, the short ∼ AD 1915–1925 period, which is characterised by a negative PDO index, is not marked by higher reconstructed SIC, but by a slight decrease in reconstructed values of SSS and SST. With respect to modern values, reconstructed SIC indicate lower values during positive PDO phases ∼ AD 1900–1910; ∼ AD 1925–1940 and ∼ AD 1980–1990. However, lower duration of SIC during periods not characterised by upwelling conditions is not systematically observable, as observed during the negative PDO period ∼ AD 1915–1925. During the older period (∼ AD 1860–1900) the link between reconstructed parameters with the large scale PDO is difficult to establish. Against PDO reconstructions (∼ AD 1860–1900), this period is characterised by a negative PDO phase but reconstructed parameters display lower SIC, higher SSS and SST conditions and low sea-surface productivity, as indicated by the low dinocyst fluxes. Therefore, results from transfer functions are not systematically associated with PDO variations along the studied period. Some of these inconsistencies may be due in part to inaccuracies of the age model. The comparison of atmospheric and paleoceanographic reconstructions is thus difficult to interpret and we cannot demonstrate with certainty that the PDO fully controls upwelling conditions and sea-surface parameters in the Mackenzie Shelf area. However, some of the reconstructed sea-surface parameters are synchronous with certain positive phases of the PDO, suggesting the probable effect of wind on sea-surface parameters and productivity at a decadal scale.

Moreover, most physical studies attributed interannual variability of the Arctic Ocean with fluctuations of the North Atlantic (NAO) and Arctic Oscillations (AO) (e.g. Deser et al., 2000; Morison et al., 2012). The AO is generally difficult to distinguish from the NAO, which is a major source of low-frequency variability. The AO switched to a positive mode around AD 1970, but showed a maximum around AD 1991 (Dickson et al., 2000; Hurrell, 1995; Hurrell and Van Loon, 1997). Our results indicate that freshwater palynomorph fluxes increased > fivefold between AD 1972 and AD 1991, from 37 specimens $cm^{-2}\,yr^{-1}$ to 202 specimens $cm^{-2}\,yr^{-1}$. Also, the maximum positive phase of the AO which began around AD 1970 coincides with a shift from a cyst of *P. dalei*-dominated dinocyst assemblage to one dominated by *O. centrocarpum* sensu lato, which is also marked in our reconstructions by a decrease of SIC duration and an increase of ∼ 1.5 °C in SST (Fig. 6b–c). In the same way, Radi et al. (2001) noticed a decrease in the relative abundance of cyst of *P. dalei* when SIC is reduced in the Chukchi Sea and Bering Strait areas. They also noted that this taxon is generally replaced by *O. centrocarpum* and *S. elongatus/frigidus* when ice conditions become important again, which is also depicted by our dinocyst assemblages (Fig. 5).

The peak in reconstructed SST and SSS values during the AD 1975–1995s period, concomitant with lower reconstructed SIC values correspond with (1) a positive phase of the PDO during AD 1979–1996; (2) a major shift in the Arctic atmospheric and oceanic circulation associated with a positive phase of the AO that began in the 1970s (Thompson and Wallace, 1998, 2000; Walsh et al., 1996). This atmospheric configuration generated an anomalously low sea level pressure in the Arctic. In the same time, satellite imagery and physico-chemical data (Macdonald et al., 1999; Parkinson et al., 1999) suggest that a strong seasonality prevailed in the marginal seas surrounding Canada Basin during the 1990s with respect to sea ice cover, with large areas of open water during the summer season and intensification of Pacific water intrusions in the Arctic during positive AO phases (McLaughin et al., 2002). However, the observed seasonality and associated reduction of sea ice extent in summer coincides with the maximum values of the Mackenzie River discharge and the maximum fluxes of freshwater palynomorphs (Fig. 4b, f). The slight similarity between the freshwater palynomorphs record (Fig. 6f) and the AO index (Fig. 6g) during the most recent phase of the freshwater palynomorph record (AD 1976–2004) would suggest a relationship between the AO and the Mackenzie freshwater discharge, but not during the previous phase (AD 1902–1976). Déry and Wood (2004) have highlighted such teleconnection between the AO with the recent decline of Hudson Bay river discharge, therefore linking the AO with the regulation of terrestrial hydrology budgets. However, Burn (2008) compared the trends in the timing of runoff of three sub-watersheds of the Mackenzie River Basin with a series of 6 climatic indices. The results showed that the AO had no effect on the timing of river runoff, suggesting that the AO has little to no effect on the hydrologic cycle in the Mackenzie Basin. On the other hand, his analysis clearly showed a link between the timing of runoff within these watersheds and the PDO index. Moreover, the oscillation that has the greatest impact on the zones located around the AO Core Region is probably the PDO (Zhao et al., 2006). At a global scale, the PDO

pattern seems to show a covariability with AO (Hetzinger et al., 2011). Thus, the series of climatic oscillations affecting the northern hemisphere are linked through a teleconnection sequence between the oceans and the atmosphere called "stadium wave" (Wyatt et al., 2011). This teleconnection plays a crucial role in climatic changes, notably in exchanges of heat fluxes within the Arctic through the Bering Strait (Woodgate et al., 2005). According to our results, the PDO pattern is closely linked with most of the sea-surface condition variability in the study area through upwelling events of Pacific origin. However, the effect of the AO cannot be totally excluded, especially with respect to freshwater inputs.

6 Conclusions

The Mackenzie Trough is characterised by a high sedimentation rate suitable for high resolution studies of paleo sea-surface conditions. The excellent preservation of palynomorphs allowed the reconstructions of sea-surface parameters. The results exposed here show that the evolution of temperature, salinity, sea ice cover and dinoflagellate productivity of the Mackenzie Trough area may be linked with the phases of the PDO at a decadal timescale. Positive phases of the PDO seem to be associated with warm, high salinity, low sea ice and high primary productivity conditions in surface waters. Conversely, negative phases are associated with cool and low salinity conditions. Freshwater palynomorphs were used to infer the evolution of local freshwater inputs, which showed three distinct phases, a dry phase in the late 19th century, and intermediate phase from AD 1900 to $\sim$1976 and probably one maximum Mackenzie River discharge phase which peaked around AD 1990. The AO does not seem to correlate with most of the parameters considered in the present study, which suggests that the Mackenzie Trough primary productivity and Mackenzie River freshwater discharge may be controlled by other parameters. The PDO may be the dominant climate oscillation mode leading oceanic circulation pattern, sea-surface parameters and productivity in the western Canadian Arctic, at least at decadal timescales.

Acknowledgements. This work was funded by the Natural Science and Engineering Research Council of Canada (NSERC) through a Discovery Grant to André Rochon, by the Institut des sciences de la mer (ISMER) and both the MALINA and ICEPROXY (ERC Stg 203441) projects. We wish to thank the officers and crew of the CCGS *Amundsen* for their help during the sampling campaign. We also thank the following people from ISMER: Étienne Faubert, Thomas Richerol, Guillaume Saint-Onge, Marc-André Cormier and Jacques Labrie; Yves Gratton and Pascal Guillot (Québec Océan) and from GEOTOP: Anne de Vernal, Taoufik Radi, Sophie Bonnet, Maryse Henry, Hans Asnong, Michèle Garneau for their help and assistance throughout the duration of this work. This is a contribution to the Malina Program.

Edited by: S. Belanger

References

Aagaard, K.: The Beaufort Undercurrent, The Alaskan Beaufort Sea: Ecosystems and Environments, Academic Press, New-York, 47–71, 1984.

Abdul Aziz, O. I. and Burn, D. H.: Trends and variability in the hydrological regime of the Mackenzie River Basin, J. Hydrol., 319, 282–294, 2006.

Appleby, P. G.: Chronostratigraphic techniques in recent sediments, in: Tracking Environmental Change Using Lake Sediments, 1, Basin Analysis, Coring, and Chronological Techniques, edited by: Last, W. M. and Smol, J. P., Kluwer Academic Publishers, Dordrecht, The Netherlands, 2001.

Barber, D. G. and Hanesiak, J. M.: Meteorogical forcing of sea ice concentrations in the southern Beaufort Sea over the period 1979–2000, J. Geophys. Res., 109, C06014, doi:10.1029/2003JC002027, 2004.

Barletta, F., St-Onge, G., Chanell, J. E. T., Rochon, A., Polyak., L., and Darby, D.: High-resolution paleomagnetic secular variation and relative paleointensity records from the western Canadian Arctic: implication for Holocene stratigraphy and geomagnetic field behavior, Can. J. Earth Sci., 45, 1265–1281, 2008.

Bjerknes, J.: A possible response of the atmospheric Hadley Circulation to equatorial anomalies of ocean temperature, Tellus, 18, 820–829, 1966.

Bjerknes, J.: Atmospheric teleconnections from the equatorial Pacific, Mon. Weather Rev., 97, 162–172, 1969.

Bjerknes, J.: Large-scale atmospheric response to the 1964–65 Pacific equatorial warming, J. Phys. Oceanogr., 2, 212–217, 1972.

Blasco, S. M., Fortin, G., Hill, P. R., O'Connor, M. J., and Brigham-Grette, J. K.: The Late Neogene and Quaternary stratigraphy of the Canadian Beaufort continental shelf, in: The Arctic Ocean region. edited by: Grantz, A., Johnson, L., and Sweeney, J. F., Geological Society of America, The Geology of North America, Vol. L, 491–502, 1990.

Blott, S. J. and Pye, K.: Gradistat: a grain size distribution and statistics package for the analysis of unconsolidated sediments, Earth Surf. Process. Landforms, 26, 1237–1248, 2001.

Bonnet, S., de Vernal, A., Hillaire-Marcel, C., Radi, T., and Husum, K.: Variability of sea-surface temperature and sea ice cover in the Fram Strait over the last two millennia, Mar. Micropaleontol., 74, 59–74, 2010.

Bonnet, S., de Vernal., A., Gersonde, R., and Lembke-Jene, L.: Modern distribution of dinocysts from the North Pacific Ocean (37–64° N, 144° E–148° W) in relation to hydrographic conditions, sea-ice and productivity, Mar. Micropaleontol., 84–85, 87–113, 2012.

Bringué, M. and Rochon, A.: Late Holocene paleoceanography and climate variability over the Mackenzie Slope (Beaufort Sea, Canadian Arctic), Mar. Geol., 291–294, 83–96, 2012.

Brohan, P., Kennedy, J., Harris, I., Tett, S. F. B., and Jones, P. D.: Uncertainty estimates in regional and global observed temperature changes: A new data set from 1850, J. Geophys. Res., 111, D12106, doi:10.1029/2005JD006548, 2006.

Burn, D. H.: Climatic influences on streamflow timing in the headwaters of the Mackenzie River Basin, J. Hydrol., 352, 225–238,

2008.
Carmack, E. C., Macdonald, R. W., and Papadakis, J. E.: Water mass structure and boundaries in the Mackenzie Shelf estuary, J. Geophys. Res., 94, 18043–18055, 1989.
Carmack, E. C. and Macdonald, R. W.: Oceanography of the Canadian Shelf of the Beaufort Sea; a setting for marine life, Arctic, 55, 29–45, 2002.
Carmack, E. C., Macdonald, R. W., and Jasper, S.: Phytoplankton productivity on the Canadian Shelf of the Beaufort Sea, Mar. Ecol. Prog. Ser., 277, 37–50, 2004.
Carson, M. A., Jasper, J. N., and Conly, F. M.: Magnitude and sources of sediment input to the Mackenzie Delta, Northwest Territories, 1974–94, Arctic, 51, 116–124, 1998.
Case, R. A. and MacDonald, G. M.: A dendroclimatic reconstruction of annual precipitation on the western Canadian prairies since A.D. 1505 from Pinus flexilus James, Quat. Res., 44, 267–275, 1995.
Cassano, E. N. and Cassano, J. J.: Synoptic forcing of precipitation in the Mackenzie and Yukon River basins, Int. J. Clim., 30, 658–674, 2010.
Coachman, L. K., Aagaard, K., and Tripp, R. B.: Bering Strait: the Regional Physical Oceanography, University of Washington Press, Seattle, 1975.
Dale, B.: Cyst formation, sedimentation, and preservation: factors affecting dinoflagellate assemblages in recent sediments from Trondheimsfjord, Norway, Rev. Palaeobot. Palynol., 22, 39–60, 1976.
Dale, B., Thorsen, T. A., and Fjellsafi, A.: Dinoflagellate cysts as indicators of cultural eutrophication in the Oslofjord, Norway, Estuar. Coast. Shelf Sci., 48, 371–382, 1999.
Danielson, S., Eisner, L., Weingartner, T., and Aagaard, K.: Thermal and haline variability over the central Bering Sea shelf: Seasonal and interannual perspectives, Cont. Shelf Res., 31, 539–554, 2011.
de Vernal, A. and Hillaire-Marcel, C.: Paléoenvironnements du Wisconsinien moyen dans l'est du Canada par l'analyse palynologique et isotopique de sédiments océaniques et continentaux, Rev. Géol. Dyn. Géogr. Phys., 27, 119–130, 1987.
de Vernal A., Henry, M., Matthiessen, J., Mudie, P. J., Rochon, A., Boessenkool, K., Eynaud, F., Grøsfjeld, K., Guiot, J., Hamel, D., Harland, R., Head, M. J., Kunz-Pirrung, M., Levac, E., Loucheur, V., Peyron, O., Pospelova, V., Radi, T., Turon, J. L., and Voronina, E.: Dinoflagellate cyst assemblages as tracers of sea-surface conditions in the northern North Atlantic, Arctic and sub-Arctic seas: the new "$n = 677$" database and application for quantitative paleoceanographical reconstruction, J. Quat. Sci., 16, 681–698, 2001.
de Vernal, A., Eynaud, F., Henry, M., Hillaire-Marcel, C., Londeix, L., Mangin, S., Matthiessen, J., Marret, F., Radi, T., Rochon, A., Solignac, S., and Turon, J. L.: Reconstruction of sea-surface conditions at middle to high latitudes of the Northern Hemisphere during the Last Glacial Maximum (LGM) based on dinoflagellate cyst assemblages, Quat. Sci. Rev., 24, 897–924, 2005.
Déry, S. J. and Wood, E. F.: Teleconnection between the Arctic Oscillation and Hudson Bay river discharge, Geophys. Res. Lett., 31, L18205, doi:10.1029/2004GL020729, 2004.
Deser, C.: On the teleconnectivity of the Arctic Oscillation, Geophys. Res. Lett., 27, 779–782, 2000.
Dickson, R. R., Osborn, T. J., Hurrell, J. W., Meincke, J., Blindheim, J., Adlandsvik, B., Vinje, T., Alekseev, G., and Maslowski, W.: The Arctic Ocean response to the North Atlantic Oscillation, J. Clim., 13, 2671–2696, 2000.
Dittmar, T. and Kattner, G.: The biogeochemistry of the river and shelf ecosystem of the Arctic Ocean: a review, Mar. Chem., 83, 103–120, 2003.
Doxaran, D., Ehn, J., Bélanger, S., Matsuoka, A., Hooker, S., and Babin, M.: Optical characterisation of suspended particles in the Mackenzie River plume (Canadian Arctic Ocean) and implications for ocean colour remote sensing, Biogeosciences, 9, 3213–3229, doi:10.5194/bg-9-3213-2012, 2012.
Fensome, R. A. and Williams, G. L.: The Lentin and Williams Index of fossil dinoflagellates (eds.) American Association of Stratigraphic Palynologists Foundation, Contr. Ser., 42, 1–909, 2004.
Government of Canada: Census of the Prairie Provinces, 1936, King's Printer, Ottawa, Canada, 1938.
Guiot, J.: Methods and programs of statistics for paleo-climatology and paleoecology, in: Quantifications des changements climatiques: methode et programmes, edited by: Guiot, J. and Labeyrie, L., Institut National des sciences de l'Univers, INSU, Monographie 1, France, Paris, 1990.
Guiot, J. and de Vernal, A.: Transfer functions: methods for quantitative paleo-ceanography based on microfossils, in: Proxies in Late Cenozoic Paleoceanography, edited by: Hillaire-Marcel, de Vernal, Elsevier, 523–563, 2007.
Guiot, J. and de Vernal, A.: Is spatial autocorrelation introducing biases in the apparent accuracy of paleoclimatic reconstructions?, Quat. Sci. Rev, 30, 2011.
Grøsfjeld, K., Harland, R., and Howe, J.: Dinoflagellate cyst assemblages inshore and offshore Svalbard reflecting their modern hydrography and climate, Norw. J. Geol., 89, 121–134, 2009.
Harland, R. and Pudsey, C. J.: Dinofagellate cysts from sediment traps deployed in the Bellingshausen, Weddell and Scotia seas, Antarctica, Mar. Micropaleontol., 37, 77–99, 1999.
Harland, R., Nordberg, K., and Filipsson, H. L.: Dinoflagellate cysts and hydrographical change in Gullmar Fjord, west coast of Sweden, Sci. Total Environ., 355, 204–231, 2006.
Hassol, S. J.: Impacts of a warming Arctic, Arctic climate impact assessment, New York, Cambridge University Press, 144 pp., 2004.
Head, M. J., Harland, R., and Matthiessen, J.: Cold marine indicators of the late Quaternary: the new dinoflagellate cyst genus Islandinium and related morphotypes, J. Quat. Sci., 16, 621–636, 2001.
Hetzinger, S., Halfar, J., Mecking, J. V., Keenlyside, N. S., Kronz, A., Steneck, R. S., Adey, W. H., and Lebednik, P. A.: Marine proxy evidence linking decadal North Pacific and Atlantic climate, Clim. Dynam., 39, 1447–1455, doi:10.1007/s00382-011-1229-4, 2011.
Heusser, L. E.: Pollen distribution in the bottom sediments of the Western North Atlantic Ocean, Mar. Micropaleontol., 8, 77–88, 1983.
Hill, P. R.: Late Quaternary sequence stratigraphy of the Mackenzie Delta, Can. J. Earth Sci., 33, 1064–1074, 1996.
Hill, P. R., Blasco, S. M., Harper, J. R., and Fissel, D. B.: Sedimentation on the Canadian Beaufort Shelf, Cont. Shelf Res., 11, 821–842, 1991.
Hill, P. R., Lewis, C. P., Desmarais, S., Kauppaymuthoo, V., and Rais, H: The Mackenzie Delta: sedimentary processes and facies

of a high-latitude, fine-grained delta, Sedimentology, 48, 1047–1078, 2001.

Howe, J. A., Harland, R., Cottier, F. R., Brand, T., Willis, K. J., Berge, J. R., Grøsfield, K., and Eriksson, A.: Dinoflagellate cysts as proxies for palaeoceanographic, Geological Society, London, Special Publications, 344, 61–74, 2010.

Hurrell, J. W: Decadal trends in the North Atlantic Oscillation: Regional temperatures and precipitation, Science, 269, 676–679, 1995.

Hurrell, J. W and van Loon, H.: Decadal variations in climate associated with the North Atlantic oscillation, Clim. Change, 36, 301–326, 1997.

IPCC (Intergovernmental Panel on Climate Change): Third assessment report, in: Climate Change 2001, edited by: Hough-ton, J. T., Ding, Y., Griggs, D. J., Noguer, M., van der Linden, P. J., Xiaosu, D., McCarthy, J., Canziani, O. F., Leary, N. A., Dokken, D. J., White, K. S., Metz, B., Davidson, O., Swart, R., Pan, J., and Watson, R. T., Cambridge University Press, Cambridge, UK, 2001.

IPCC (Intergovernmental Panel on Climate Change): Climate Change 2007: Synthesis Report: http://www.ipcc.ch/pdf/assessment-report/ar4/syr/ar4_syr.pdf, 2007.

Iseki, K., Macdonald, R. W., and Carmack, E.: Distribution of particulate matter in the southeastern Beaufort Sea in late summer, Polar Biol., 1, 35–46, 1987.

Jerosch, K.: Geostatistical mapping and spatial variability of surficial sediment types on the Beaufort Shelf based on grain size data, J. Mar. Syst., in press, 2012.

Kulikov, E. A., Carmack, E. C., and Macdonald, R. W.: Flow variability at the continental shelf break of the Mackenzie Shelf in the Beaufort Sea, J. Geophys. Res., 103, 12725–12741, 1998.

Kunz-Pirrung, M.: Dinoflagellate cyst assemblages in surface sediments of the Laptev Sea region (Arctic OCean) and their relationship to hydrographic conditions, J. Quat. Sci., 16, 637–649, 2001.

Ledu, D., Rochon, A., de Vernal, A., and St-Onge, G.: Palynological evidence of Holocene climate change in the eastern Arctic: a possible shift in the Arctic oscillation at the millennial time scale, Can. J. Earth Sci., 45, 1363–1375, 2008.

Ledu, D., Rochon, A., de Vernal, A., and St-Onge, G.: Holocene paleoceanography of the Northwest Passage, Canadian Arctic Archipelago, Quat. Sci. Rev, 29, 3468–3488, 2010a.

Ledu, D., Rochon, A., de Vernal, A., Barletta, F., and St-Onge, G.: Holocene sea-ice history and climate variability along the main axis of the Northwest Passage, Canadian Arctic, Paleoceanography, 25, PA2213, doi:10.1029/2009PA001817, 2010b.

Macdonald, R. W., Wong, C. S., and Erickson, P. E.: The distribution of nutrients in the southeastern Beaufort Sea: Implications for water circulation and primary production, J. Geophys. Res.-Oceans, 92, 2939–2952, 1987.

Macdonald, R. W., Paton, D. W., Carmack, E. C., and Omstedt, A.: The freshwater budget and under-ice spreading of Mackenzie River water in the Canadian Beaufort Sea based on salinity and $^{18}O/^{16}O$ measurements in water and ice, J. Geophys. Res., 100, 895–919, 1995.

Macdonald, R. W., Solomon, S. M., Cranston, R. E., Welch, H. E., Yunker, M. B., and Gobeil, C.: A sediment and organic carbon budget for the Canadian Beaufort Shelf, Mar. Geol., 144, 255–273, 1998.

Macdonald, R. W., Carmack, E. C., McLaughlin, F. A., Falkner, K. K., and Swift, J. H.: Connections among ice, runoff and atmospheric forcing in the Beaufort Gyre, Geophys. Res. Lett., 26, 2223–2226, 1999.

Macdonald, R. W., McLaughlin, F. A., and Carmack, E. C.: Freshwater and its sources during the SHEBA drift in the Canada Basin of the Arctic Ocean, Deep-Sea Res. I, 49, 1769–1785, 2002.

Macdonald, R. W., Harner, T., and Fyfe, J.: Recent climate change in the Arctic and its impact on contaminant pathways and interpretation of temporal trend data, Sci. Total Environ., 342, 5–86, 2005.

Mantua, N. J., Hare, S. R., Zhang, Y., Wallace, J., and Francis R.: A Pacific interdecadal climate oscillation with impact on salmon production, Bull. Amer. Meteor. Soc., 78, 1069–1079, 1997.

Mantua, N. J. and Hare, S. R.: The Pacific decadal oscillation, J. Oceanogr., 58, 35–44, 2002.

Martin, J., Tremblay, J.-É., Gagnon, J., Tremblay, G., Lapoussière, A., Jose, C., Poulin, M., Gosselin, M., Gratton, Y., and Michel, C.: Prevalence, structure and properties of subsurface chlorophyll maxima in Canadian Arctic waters, Mar. Ecol. Prog. Ser., 412, 69–84, 2010.

Marret, F. J., Eiríksson, J., Knudsen, K.-L., and Scourse, J.: Distribution of dinoflagellate cyst assemblages in surface sediments from the northern and western shelf of Iceland, Rev. Palaeobot. Palynol., 128, 35–54, 2004.

Matsuoka, A., Bricaud, A., Benner, R., Para, J., Sempéré, R., Prieur, L., Bélanger, S., and Babin, M.: Tracing the transport of colored dissolved organic matter in water masses of the Southern Beaufort Sea: relationship with hydrographic characteristics, Biogeosciences, 9, 925–940, doi:10.5194/bg-9-925-2012, 2012.

Matthews, J.: The assessement of a method for the determina-tion of absolute pollen frequencies, The New Phytologist, 68, 161–166, 1969.

Matthiessen, J., Kunz-Pirrung, M., and Mudie, P. J.: Freshwater chlorophycean algae in recent marine sediments of the Beaufort, Laptev and Kara Seas (Arctic Ocean) as indicators of river runoff, Int. J. Earth Sci., 89, 470–485, 2000.

Matthiessen, J., de Vernal, A., Head, M., Okolodkov, Y., Zonneveld, K., and Harland, R.: Modern organic-walled dinoflagellate cysts in Arctic marine environments and their (paleo-) environmental significance, Palaontologische Zeitschrift, 79, 3–51, 2005.

McBean, G., Alekseev, G., Chen, D., Førland, E., Fyfe, J., Groisman, P. Y., King, R., Melling, H., Vose, R., and Whitfield, P. H.: Arctic climate: past and present, Arctic climate impact assessment, Scientific Report, Cambridge University Press, 2005.

Melling, H.: Hydrographic changes in the Canada Basin of the Arctic Ocean, 1979–1996, J. Geophys. Res., 103, 7637–7645, 1998.

McLaughin, F., Carmack, E., and Macdonald, R.: The Canada Basin, 1989–1995: Upstream events and far-field effects of the Barents Sea, J. Geophys. Res., 107, C7, doi:10.1029/2001JC000904, 2002.

Minobe, S.: A 50–70 year climatic oscillation over the North Pacific and North America, Geophys. Res. Lett., 24, 683–686, 1997.

Moore, G. W. K., Holdsworth, G., and Alverson, K.: The impact that elevation has on the ENSO signal in precipitation records from the Gulf of Alaska Region, Clim. Change, 59, 101–121, 2003.

Morison, J., Kwok, R., Peralta-Ferriz, C., Alkire, M., Rigor, I., Andersen, R., and Steele, M.: Changing Arctic Ocean freshwater

pathways Nature, 481, 66–70, 2012.
Mucci, A., Lansard, B., Miller, L. A., and Papakyriakou, T. N.: CO_2 fluxes across the air sea interface in the southeastern Beaufort Sea: Ice-free period, J. Geophys. Res., 115, C04003, doi:10.1029/2009JC005330, 2010.
Mudie, P. J.: Pollen distribution in recent marine sediments, Eastern Canada, Can. J. Earth Sci., 19, 729–747, 1982.
Mudie, P. J. and Rochon, A.: Distribution of dinoflagellate cysts in the Canadian Arctic marine region, J. Quat. Sci., 16, 603–620, 2001.
Nikolopoulos, A., Pickart, R. S., Fratantoni, P. S., Shimada, K., Torres, D. J., and Jones, E. P.: The western arctic boundary current at 152° W: structure, variability, and transport, Deep-Sea Res. II, 56, 1164–1181, 2009.
Niebauer, H. J. and Day, R. H.: Causes of interannual variability in the sea ice cover of the eastern Bering Sea, GeoJournal, 18, 45–59, 1989.
Niebauer, H. J.: Variability in Bering Sea ice cover as affected by a regime shift in the North Pacific in the period 1947–1996, J. Geophys. Res. C, 103, 717–727, 1998.
NODC: World Ocean Atlas, National Oceanographie Center, National Oceanic and Atmospheric Administration, Boulder, CO, CD-Rom data Sets, 2001.
O'Brien, M. C., Macdonald, R. W., Melling, H., and Iseki, K.: Particle fluxes and geochemistry on the Canadian Beaufort Shelf: implications for sediment transport and deposition, Cont. Shelf Res., 26, 41–81, 2006.
Okkonen, S., Ashjian, C. A., Campbell, R. G., Maslowski, W., Clement- Kinney, J., and Potter, R.: Intrusion of warm Bering/Chukchi waters onto the shelf in the western Beaufort Sea, J. Geophys. Res., 114, C00A11, doi:10.1029/2008JC004870, 2009.
Overland, J., Adams, J., and Bond, N.: Decadal variability of the Aleutian Low and its relation to high-latitude circulation, J. Climate, 12, 1542–1548, 1999.
Parkinson, C. L., Cavalieri, D. J., Gloersen, P., Zwally, H. J., and Comiso, J. C.: Arctic sea ice extents, areas, and trends, 1978–1996, J. Geophys. Res., 104, 20837–20856, doi:10.1029/1999JC900082, 1999.
Pelletier, B. R.: Marine science atlas of the Beaufort Sea sediments, Geological Survey of Canada, Miscellaneous Report 38, 27 pp., 1984.
Persson, A., Godhe, A., and Karlson, B.: Dinoflagellate cysts in recent sediments from the west coast of Sweden, Botanica Marina, 43, 69–79, 2000.
Pickart, R. S., Moore, G. W. K., Torres, D. J., Fratantoni, P. S., Goldsmith, R. A., and Yang, J.: Upwelling on the continental slope of the Alaskan Beaufort Sea: Storms, ice, and oceanographic response, J. Geophys. Res., 114, C00A13, doi:10.1029/2008JC005009, 2009.
Pisaric, M. F. J., Sean, K. C., Kokeli, S. V., and Youngblut, D.: Anomalous 20th century tree growth, Mackenzie Delta, Northwest Territories, Canada, Geophys. Res. Lett., 34, l05714, doi:10.1029/2006GL029139, 2007.
Pisaric, M. F. J., St-Onge, S. M., and Kokelj, S. V.: Tree-ring Reconstruction of Early-growing Season Precipitation from Yellowknife, Northwest Territories, Canada, Arct. Antarct. Alp. Res., 41, 486–496, 2009.
Polyakov, I. V., Alekseev, G. V., Bekryaev, R. V., Bhatt, U., Colony, R. L., Johnson, M. A., Karklin, V. P., Makshtas, A. P., Walsh, D., and Yulin, A. V.: Observationally based assessment of polar amplification of global warming, Geophys. Res. Lett., 29, 1878, doi:10.1029/2001GL011111, 2002.
Porter, T. J., Pisaric, M. F. J., Kokelj, S. V., and Edwards, T. W. D.: Climatic Signals in ^{13}C and ^{18}O of Tree-rings from White Spruce in the Mackenzie Delta Region, Northern Canada, Arct. Antarct. Alp. Res., 41, 497–505, 2009.
Prell, W. L.: The stability of low-latitude sea-surface temperatures, an evaluation of the CLIMAP reconstruction with emphasis on the positive SST anomalies, Report TR025, US Dep. of Energy, Washington, DC, 1985.
Radi, T., de Vernal, A., and Peyron, O.: Relationships beetween dinoflagellate cyst assemblages in surface sediment and hydrographic conditions in the Bering and Chukchi seas, J. Quat. Sci., 16, 667–680, 2001.
Radi, T., Pospelova, V., de Vernal, A., and Barrie, J. V.: Dinoflagellate cysts as indicators of water quality and productivity in estuarine environments of British Columbia, Mar. Micropaleontol., 62, 269–297, 2007.
Radi, T., Bonnet, S., Cormier, M. A., de Vernal, A., Durantou, L., Faubert, E., Head, M. J., Henry, M., Pospelova, V., Rochon, A., and Van Nieuwenhove, N.: Operational taxonomy for round, brown, spiny dinocysts from high latitudes of the Northern Hemisphere, Mar. Micropaleontol., in press, 2012.
Rawlins, M. A., Steele, M., Serreze, M. C., Vorosmarty, C. J., Ermold, W., Lammers, R. B., McDonald, K. C., Pavelsky, T. M., Shilomanov, A., and Zhang, J.: Tracing freshwater anomalies through the air-land-ocean system: A case study from the Mackenzie River Basin and the Beaufort Gyre, Atmos. Ocean., 47, 79–97, 2009.
Richerol, T., Rochon, A., Blasco, S., Scott, D. B., Schell, T. M., and Bennett, R. J.: Evolution of paleo sea-surface conditions over the last 600 years in the Mackenzie Trough, Beaufort Sea (Canada), Mar. Micropaleontol., 68, 6–20, 2008a.
Richerol, T., Rochon, A., Blasco, S., Scott, D. B., Schell, T. M., and Bennett, R. J.: Distribution of dinoflagellate cysts in surface sediments of the Mackenzie Shelf and Amundsen Gulf, Beauford Sea (Canada), J. Marine Syst., 74, 825–39, 2008b.
Rochon, A. and de Vernal, A.: Palynomorph distribution in Recent sediments from the Labrador Sea, Can. J. Earth Sci., 31, 115–127, 1994.
Rochon, A., de Vernal, A., Turon, J. L., Matthiessen, J., and Head, M. J.: Distribution of recent dinoflagellate cysts in surface sediments from the North Atlantic Ocean and adjacent seas in relation to sea-surface parameters, (eds.) American Association of Stratigraphic Palynologists Foundation, Dallas, Texas, Contr. Ser., 35, 1–152, 1999.
Sanchez-Cabeza, J. A. and Ruiz-Fernández, A. C.: ^{210}Pb sediment radiochronology: An integrated formulation and classification of dating models, Geochim. Cosmochim. Ac., 82, 183–200, 2012.
Sauchyn, D. J. and Beaudoin, A. B.: Recent environmental change in the southwestern Canadian plains, The Canadian Geographer, 42, 337–353, 1998.
Sauchyn, D. J. and Skinner, W. R.: A Proxy Record of Drought Severity for the Southwestern Canadian Plains, Can. Water Resour. J., 26, 253–272, 2001.

Schneider, N. and Cornuelle, B. D.: The forcing of the PDO, J. Climate, 18, 4355–4373, 2005.

Scott, D. B., Schell, T., Rochon, A., and Blasco, S.: Benthic foraminifera in the surface sediments of the Beaufort Shelf and Slope, Beaufort Sea, Canada: Applications and implications for past sea-ice conditions, J. Mar. Syst., 74, 840–863, doi:10.1016/j.jmarsys.2008.01.008, 2008.

Scott, D. B., Schell, T., St-Onge, G., Rochon, A., and Blasco, B.: Foraminiferal assemblage changes over the last 15,000 years on the Mackenzie-Beaufort Sea Slope and Amundsen Gulf, Canada: Implications for past sea ice conditions, Paleoceanography, 24, PA2219, doi:10.1029/2007PA001575, 2009.

Solignac, S., Grøsfjeld, K., Giraudeau, J., and de Vernal, A.: A Distribution of modern dinocyst assemblages in the western barents sea, Norw. J. Geol., 88, 109–119, 2009.

Schmidt, S., Howa, H., Mouret, A., Lombard, F., Anschutz, P., and Labeyrie, L.: Particle fluxes and recent sediment accumulation on the Aquitanian margin of Bay of Biscay, Cont. Shelf Res., 29, 1044–1052, 2009.

Steele, M. and Ermold, W.: Salinity trends on the Siberain shelves, Geophys. Res. Lett., 31, L24308, doi:10.1029/2004GL021302, 2004.

Stockton, C. W. and Fritts, H. C.: Long-term reconstruction of water level changes for Lake Athabasca by analysis of tree-rings, Water Resour. Bull., 9, 1006–1027, 1973.

St George, S., Meko, D. M., Girardin, M. P., MacDonald, G. M., Nielsen, E., Pederson, G. T., Sauchyn, D. J., Tardif, J. C., and Watson, E.: The tree-ring record of drought on the Canadian Prairies, J. Climate, 22, 689–710, doi:10.1175/2008JCLI2441.1, 2009.

Susek, E., Zonneveld, K. A. T., Fischer, G., Versteegh, G. J. M., and Willems, R.: Orgnaic-walled dinoflagellate cyst production in relation to upwelling intensity and lithogenic influx in the Cape Blanc region (off north-west Africa), Phycol. Res., 53, 97–112, 2005.

Thompson, D. W. J. and Wallace, J. M.: The Arctic Oscillation signature in the wintertime geopotential height and temperature fields, Geophys. Res. Lett., 25, 1297–1300, 1998.

Thompson, D. W. J. and Wallace J. W.: Annual modes in the extratropical circulation, Part I: Month to month variability, J. Climate, 13, 1000–1016, 2000.

Tremblay, J. E., Bélanger, S., Barber, D. G., Asplin, M., Martin, J., Darnis, G., Fortier, L., Gratton, Y., Link, H., Archambault, P., Sallon, A., Michel, C., Williams, W. G., Philippe, B., and Gosselin M.: Climate forcing multiplies biological productivity in the coastal Arctic Ocean, Geophys. Res. Lett., 38, L18604, doi:10.1029/2011GL048825, 2011.

UNSCEAR: Sources and effects of ionizing radiation, UNSCEAR 2000 report to the General Assembly, with scientific annexes, Sources, New York, United Nations, 1, 1–654, 2000.

Walsh, J. E., Tanaka, H. L., and Weller, G.: Wadati conference on global change and the polar climate, 7–10 November 1995, Tsukuba, Japan, Bull. Am. Meteor. Soc., 77, 1268–1273, 1996.

Wang, J., Cota, G. F., and Comiso, J. C.: Phytoplankton in the Beaufort and Chukchi seas; distribution, dynamics, and environmental forcing, Deep-Sea Res. II, 52, 3355–3368, 2005.

Watson, E. and Luckman, B. H.: Long hydroclimate records from tree-rings in western Canada: Potential, problems and prospects, Can. Water Resour. J., 31, 205–228, 2006.

Wendler, G., Shulski, M., and Moore, B.: Changes in the climate of the Alaskan North Slope and the ice concentration of the adjacent Beaufort Sea, Theor. Appl. Climatol., 99, 67–74, 2009.

Williams, W. J., Carmack, E. C., Shimada, K., Melling, H., Aagaard, K., Macdonald, R. W., and Ingram, R. G.: Joint effects of wind and ice motion in forcing upwelling in Mackenzie Trough, Beaufort Sea, Cont. Shelf Res., 26, 2352–2366, 2006.

Woodgate, R. A. and Aagaard, K.: Revising the Bering Strait freshwater flux into the Arctic Ocean, Geophys. Res. Lett., 32, L02602, doi:10.1029/2004GL021747, 2005.

Wyatt, M., Kravtsov, S., and Tsonis, A. A.: Atlantic Multidecadal Oscillation and Northern Hemisphere's climate variability, Clim. Dynam., doi:10.1007/s00382-011-1071-8, 2011.

Zhao, J. P., Cao, Y., and Shi, J. X.: Core region of Arctic Oscillation and the main atmospheric events impact on the Arctic, Geophys. Res. Lett., 33, L22708, doi:10.1029/2006GL027590, 2006.

Zonneveld, K. A. F., Versteegh, G. J. M., and de Lange, G. J.: Preservation of organic walled dinoflagellate cysts in different oxygen regimes: a 10 000 years natural experiment, Mar. Micropaleontol., 29, 393–405, 1997.

Zonneveld, K. A. F. and Brummer, G. A.: (Palaeo-)ecological significance, transport and preservation of organic walled dinoflagellate cysts in the Somali Basin, NW Arabian Sea, Deep-Sea Res. II, 47, 2229–2256, 2000.